Available online at www.sciencedirect.com

SciVerse ScienceDirect

Procedia Engineering 36 (2012) 186 – 194

Procedia Engineering

www.elsevier.com/locate/procedia

IUMRS-ICA 2011

# Controlled Morphological Structure of Ceria Nanoparticles Prepared by Spray Pyrolysis

Shao-Ju Shih[a*], Ying-Ying Wu[a], Chin-Yi Chen[b] and Chin-Yang Yu[a]

[a]*Department of Materials Science and Engineering, National Taiwan University of Science and Technology, 43, Keelung Road, Sec. 4, Taipei,10607, Taiwan, ROC.*

[b]*Department of Materials Science and Engineering, Feng Chia University, 100, Wenhwa Road, Taichung, 40724, Taiwan, ROC.*

**Abstract**

Ceria based materials have been widely used as catalyst supporters and electrolytes. Different applications require different morphologies, and the microstructural control during the synthesis is crucial. In the study, ceria particles were prepared from various precursors using a spray pyrolysis (SP). Comparing to the hollow and porous particles, the formation mechanism with solid spherical structure is not clarified readily. The ceria particles were characterized by transmission electron microscopy, thermogravimetry analysis and X-ray photoelectron spectroscopy. This experimental result suggests that the morphology is controlled by the precursors and could be related to their decomposed behavior during the heating process in SP.



*Keywords*: Ceria; spray pyrolysis; transmission electron microscopy; thermogravimetric analysis; X-ray photoelectron spectroscopy

## 1. Introduction

Ceria-based materials have been extensively applied in catalyst supports [1], CO reduction catalysts [2, 3] and solid-oxide-fuel-cell (SOFC) electrolytes [4] because of their superior properties of thermal stability [5], oxygen storage capacity [3] and ion conductivity [4, 6]. For different applications, different morphologies of ceria particles are needed [1-4]. For example, initially, as a catalyst support, ceria-based materials need the porous structure [1] with higher surface area to increases the loading amount of catalysts for higher reaction efficiency. Secondly, for the catalysts in CO oxidation, the ceria hollow structure has advantages because their interior space and loose shell structure are expected to enhance the spatial dispersion for higher gas adsorption [3]. Finally, the SOFC electrolytes must to be dense to prevent gas mixing, and ceria spherical particles have less pores to be removed than hollow/porous particles for

* Corresponding author. Tel.: +886-2-2730-3716; Fax: +886-2-2737-6544.
*E-mail address*: shao-ju.shih@mail.ntust.edu.tw.

1877-7058 
doi:10.1016/j.proeng.2012.03.029

densification processes. Thus, morphology control in ceria-based particles is crucial for industrial applications.

There are a number of preparation methods for ceria-based particles, e.g. sol-gel [7], micro-emulsion [8], precipitation [9] and spray pyrolysis (SP) [10, 11]. SP process has been chosen because of great potentials with low cost, continues process and chemistry flexibility [12, 13]. For the SP process, different particle morphologies are influenced by surface precipitation (for hollow and porous particles) or volume precipitation mechanisms (for solid spherical particles) of the solute during drying [12]. For ceria particles prepared from the SP process, the morphologies of hollow and porous were frequently observed rather than solid spherical particles because of fast evaporation rate and lack of time for solute diffusion and particle densification [11, 14]. In order to obtain spherical particles, several methods from physical and chemical approaches were proposed [14-19].

For physical approaches, increasing evaporation time and decreasing the distance of solute diffusion are common strategies. First, for adjusting evaporation process, Dubois et al. [15] used a furnace with a thermal gradient, which provides a series temperatures for a longer evaporation period, to generate solid spherical yttra-stabilized zirconia particles from the precursor solution (3 mol%) of $ZrOCl_2 \cdot 8H_2O$ and $Y(NO_3)_3 \cdot 5H_2O$. Second, for shorten diffusion distance of solute (smaller droplet or particle sizes), Zhang and Messing [14] prepared the low concentration precursor solutions (0.044~0.057M) of $ZrOCl_2 \cdot 8H_2O$ or ZrO(OH)Cl to produce solid zirconia particles. Also, our previous works [16, 17] discovered the small portion of solid spherical ceria particles (particle diameters less than ~100 nm) and the hollow and porous particles (particle diameters larger than ~100 nm), using the precursor solutions (1wt%) of $Ce(NO_3)_3 \cdot 6H_2O$ or $Ce(C_2H_3O_2)_3 \cdot 1.5H_2O$. On the other hand, for chemical approaches, the concept of precursor modification was applied. Ishizawa et al. [18] applied the metal alkoxides to produce three-dimensional polymer networks to avoid the rupture of the solid spherical particles during solvent evaporation for solid spherical particles. Xu et al. [19] used two precursors of $Ce(NO_3)_3$ and $Ce(C_2H_3O_2)_3$ to fabricate solid spherical ceria particles. From previous results, although solid spherical particles can be obtained, these methods contain some disadvantages (e.g. rigorous operating conditions [15], limitation of particle size [14, 16, 17], high-cost metal-organic slats [18] and multi-precursors [19]), which needs to be overcome.

We proposed a straightforward method by using a single-precursor with different solubility behaviors to change particle morphologies. Three precursors: cerium (IV) ammonium nitrate (CeAN), cerium (III) acetate hydrate (CeA) and cerium (III) nitrate hydrate (CeN) were chosen because they are commercially available. For the first type, the solubilities of CeAN and CeN increase with increasing temperature of 1409 g/L at 25$^{o}$C and 2268 g/L at 85.6$^{o}$C [20] for CeAN and 637 g/L at 25$^{o}$C and 739 g/L at 50$^{o}$C [21] for CeN, respectively. For the second type, the solubility of CeA decreases with increasing temperature from 115 g/L at 15$^{o}$C to 100 g/L at 25$^{o}$C [22]. The solubilities of CeAN and CeN increase with increasing temperature. This is possibly due to the relatively strong hydrophilic properties of both cerium complexes comparing to CeA.

In the present study, we examined morphologies and particle diameter distributions of ceria particles of the three precursors (CeAN, CeA and CeN) by transmission electron microscopy (TEM), and identify the phase of the particles by selected area electron diffraction (SAED). The formation mechanisms for different morphological ceria nanoparticles by SP were proposed. Then, the decomposition behaviors of the three precursors were examined by thermogravimetric analysis (TGA) and were correlated with the related morphologies. In addition, since the Ce(III)/Ce(IV) couple are related to oxygen storage capacity properties [23], total concentrations of Ce (III) in the ceria particles from three different precursors were examined using X-ray photoelectron spectroscopy (XPS).

## 2. Experimental Procedure

### *2.1. Powder preparation*

Ceria particles were prepared using a laboratory-scale SP electrostatic deposition system. Details of the experimental procedures were described elsewhere [24, 25]. In the SP process the precursor solution was first atomized into small droplets while an air flow with a controlled flow rate carried the droplets into the heated tubular reactor (The temperatures of the three heating zones are 250, 650 and 350$^{o}$C). In the reactor the droplets undergo solvent evaporation, solute precipitation and precursor decomposition to convert into oxide particles. The resulting particles were then collected by a cylindrical electrostatic collector with an applied high-voltage potential of -16 kV. The three precursors used for generation of ceria powders were de-ionized water solutions (1 wt%) of, cerium (IV) ammonium nitrate, $(NH_4)_2Ce(NO_3)_6$ (99.5%, Alfa Aesar, Johnson Matthey Co.), cerium (III) acetate hydrate, $Ce(C_2H_3O_2)_3$•$1.5H_2O$ (99.9%, Alfa Aesar, Johnson Matthey Co.) and cerium (III) nitrate hydrate, $Ce(NO_3)_3$•$6H_2O$ (99.5%, Alfa Aesar, Johnson Matthey Co.).

### *2.2. Characterization*

TEM specimens were prepared by dispersing the particles in high-purity ethanol using an ultrasonic bath for around 5 min, and then depositing a drop of suspension onto a holey carbon film grid. The solvent on the carbon grid was evaporated at room temperature. A JEOL 3000F (FEG) TEM operated at 297 keV was used to examine the particle morphology. Imaging of ceria particles was carried out using a high resolution TEM (JEM-3000F, JEOL, Japan) with electron energy of 300 keV. The crystallographic structures of three particles are characterized by SAED from random selected particles with an aperture size of 800 nm. The particle diameters of three ceria powders (from CeAN, CeA and CeN) were measured from a number of TEM micrographs which included over 100 particles.

The three precursors, CeA, CeN and CeAN, were characterized by TGA (TGA, Perkin-Elmer Model TGA-7) under an ambient airflow to remove decomposition products. The heating rate was 40$^{o}$C/min.

The XPS measurements for the three ceria powders were performed with a Versa-Probe ESCA spectrometer (PHI 5000, Physical Electronics Inc., USA) using monochromated Al-K$\alpha$ X-ray source (1486.6 eV, 15 mA, and 0.3 mm spot). The high resolution multiplex scans of Ce-3d were taken with a 0.1 eV step and 25 eV analyzer pass energy and repeated for forty times. All samples were cleaved in vacuum at a base pressure of $5 \times 10^{-5}$ Torr. Curve fitting was carried out by the Multipax software (V8.2c, Vlvac-Phi Inc., USA). The spectra were corrected using Shirley background. All peaks in the spectra were fitted with a Gaussian–Lorentzian shape function to deconvolute overlapping peaks. Peak positions were calibrated by the C-1s peak (284.5 eV) of carbon from carbon tape, which supported the particles.

## 3. Results and Discussion

### *3.1. Particle morphology*

Figures 1 (a), (b) and (c) show the TEM images of the three type ceria particles prepared by SP from CeAN, CeA and CeN, respectively. Surprisingly, the particles prepared from CeAN are all solid spherical (see Fig. 1 (a)). The reason for that may due to good solubility of CeAN in aqueous solution that the ammonium nitrate act as a surfactant to form micelles. This causes the ammonium nitrate and water surrounded outside of the cerium, known as the formation mechanism of volume precipitation of cerium [25], before the SP proceeded. The ceria particles prepared from CeA mainly showed the hollow

structures of open pores (see Fig. 1(b)) due to the formation of surface precipitation [12] before extraction of non-metallic moieties. The structure of close pores which was prepared by SP of CeN precursor was shown in Fig. 1 (c). The solubility of CeN precursor is between the aqueous solution made by CeAN and by CeA. The formation of particle structures was therefore involved both volume precipitation and surface precipitation resulting in the close-pore hollow spherical particles. Further detail about the formation mechanism of the morphology of ceria particles from three precursors was shown in Fig. 2.

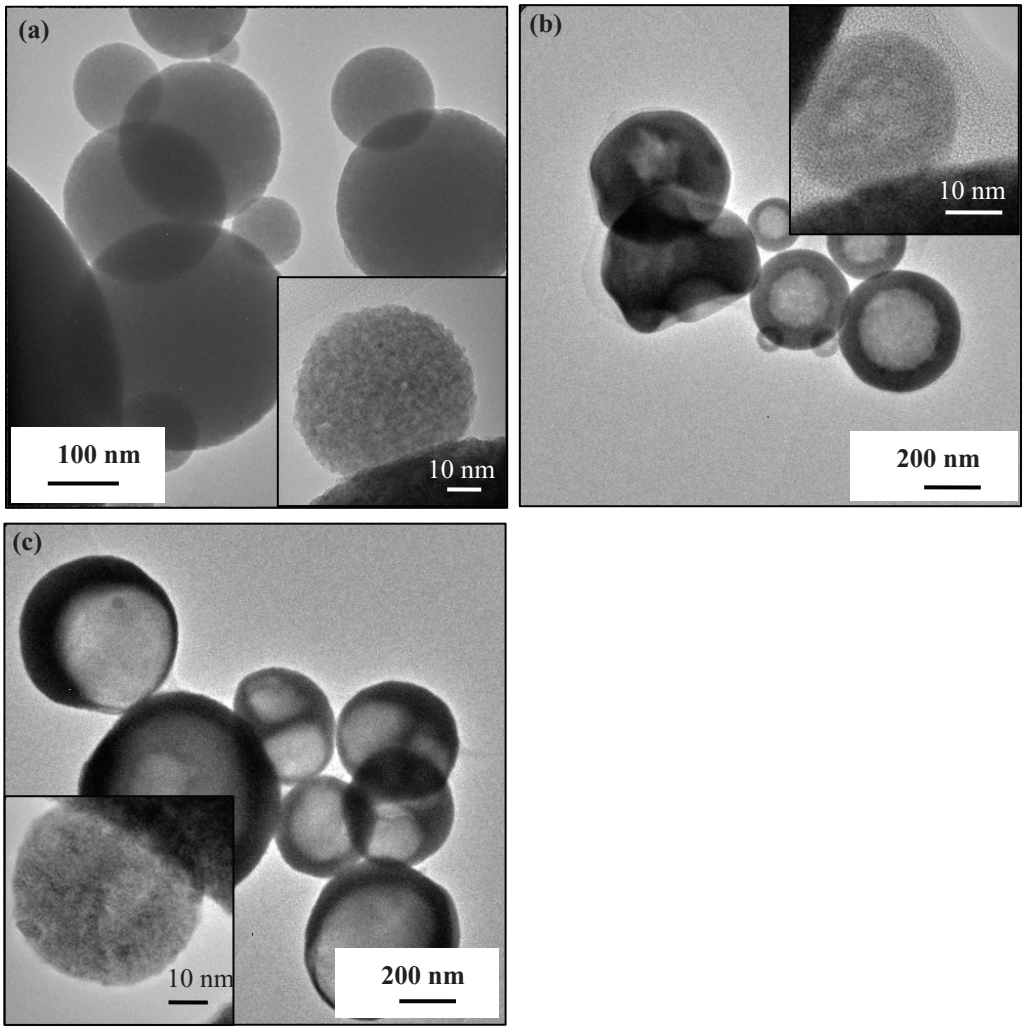


Fig. 1. TEM images of ceria particles prepared from (a) CeAN, (b) CeA and (c) CeN. High resolution images of an ceria particle are shown in the down-right, up-left corner and down-left corner of (a), (b) and (c), respectively.

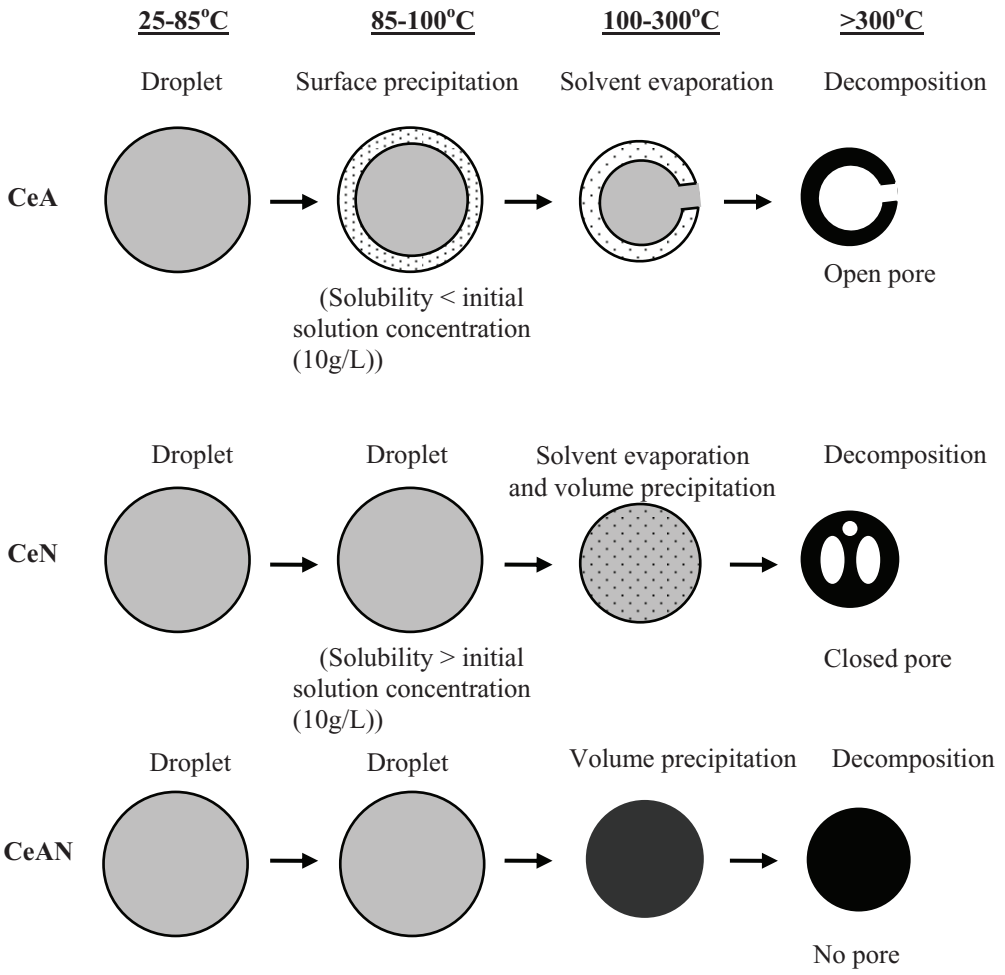


Fig. 2. The schematic diagram illustrating the formation mechanism of the morphologies of ceria particles from the three precursors (CeA, CeN and CeAN) by SP.

By the statistical analysis, the average diameters of ceria particles prepared from CeAN, CeA and CeN are 204 ± 131 nm, 344 ± 183 nm and 304 ± 182 nm. Combing morphology and particle diameter analysis, unlike the particles prepared from CeAN, the morphology of the particles prepared from CeA and CeN is a function of particle diameter. Solid spherical particles can be observed with particle diameter 61 ± 16 nm prepared from CeA and 35 ± 7 nm prepared from CeN; hollow spherical particles with particle diameter 139 ± 38 nm prepared from CeA and 216 ± 123 nm prepared from CeN; and hollow concave particles with particle diameter of 421 ±126 nm prepared from CeA and 597 ± 101 nm. More details have been showed three main morphologies prepared from CeA and CeN precursors [16]. Based on previous studies [24-26], the smaller particles having shorter solute diffusion distance comparing to larger particles are solid due to volume precipitation; nevertheless, the larger particles are hollow because of surface precipitation [12]. For the hollow particles, the surfaces of the hollow concave particles are rougher than

that of the hollow spherical particles because of different stress formation in the cooling process, which is discussed in the early study [25].

For the hollow particles, the main difference between the CeA and CeN ceria particles is the pore structure. According to the result of electron tomography [17], the particles from CeA contain some open pores, but the particles from CeN contain all close pores, which supported by the surface area measurement. The BET result shows that the surface area (62.03 $m^2/g$) of the CeA ceria particles is twice larger than that (30.89 $m^2/g$) of the CeN ceria particles, but there is no much difference in particle diameter for the CeA and CeN ceria particles (344 ± 183 nm for CeA; 304 ± 182 nm for CeN).

### *3.2. Thermal analysis of cerium complexes*

TGA for cerium complexes, CeA, CeN and CeAN, is shown in Fig. 3. CeA exhibited highest thermal stability with only 5% weight loss before 320°C. This is expected as that the acetate group has higher tolerance in temperature than the others. Clearly, all complexes exhibited one major step in the loss of mass due to the decomposition of non-metallic moieties. The decomposition temperature was found at 320°C for CeA, 250°C for CeN and 220°C for CeAN which was slightly decreased the decomposition temperature. The three types of ceria were observed after decomposed above 800°C under the atmosphere. These can be assigned to the loss of acetate hydrate for CeA, nitrate hydrate for CeN and ammonium nitrate for CeAN. The remaining weight percents of three cerium dioxides (53% from CeA, 41% from CeN and 25% from CeAN) were very close to that expected value (49% from CeA, 36% from CeN and 30% from CeAN).

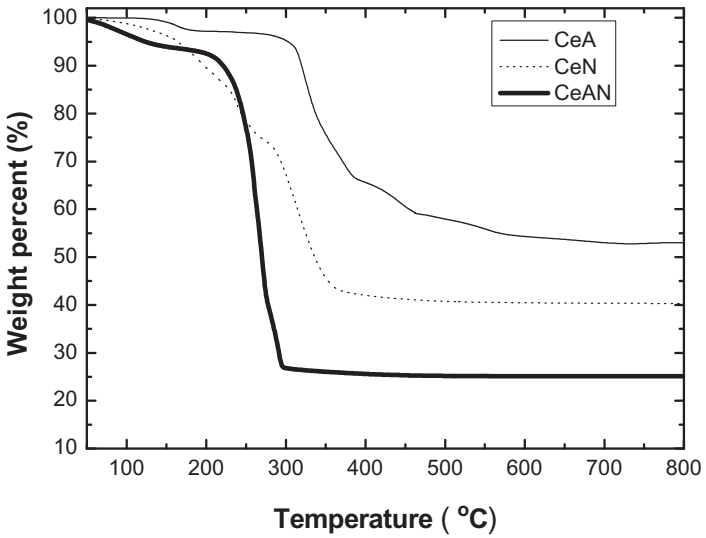


Fig. 3. The schematic diagram illustrating the formation mechanism of the morphologies of ceria particles from the three precursors (CeA, CeN and CeAN) by SP.

### *3.3. Concentration of cerium (III)*

Figure 4 illustrates the XPS Ce-3d spectrum (after background subtraction) for the ceria particles, as an example. The spectrum consists of eight peaks [27,28], four doublets denoted as $V/U$, $V'/U'$, $V''/U''$ and $V'''/U'''$. Based on the convention establish by Burroughs [27] et al. peaks $V'$ and $U'$ refer to $3d_{3/2}$ and $3d_{5/2}$ of Ce (III), respectively; peaks $V/V''/V'''$ and $U/U''/U'''$ refer to $3d_{3/2}$ and $3d_{5/2}$ of Ce (IV), respectively. The results from fitting (position and area) for these eights peaks are listed. Using the method developed by El Fallah et al. [29], the fitted peak areas in the XPS spectrum of Ce-3d (Fig. 4) can be used to estimate the concentration of Ce (III) by the following equation [28],

$$[Ce(III)] = \frac{V' + U'}{V + U + V' + U' + V'' + U'' + V''' + U'''} \quad (1)$$

The calculated Ce (III) concentrations of the ceria particles from CeAN, CeA and CeN show that, as expected, the [Ce (III)] from the particles prepared from CeA and CeN are 17.71% and 17.72%, respectively, higher than that of 14.55% from CeAN. The [Ce (III)] difference between the ceria particles from the precursors of Ce (III) and the precursors of Ce (IV) is ~3%, which is not significant comparing to the difference doped and un-doped ceria particles (~19% for $CeO_2$ and $Ce_{0.8}Zr_{0.2}O_{2-x}$ particles) [23].

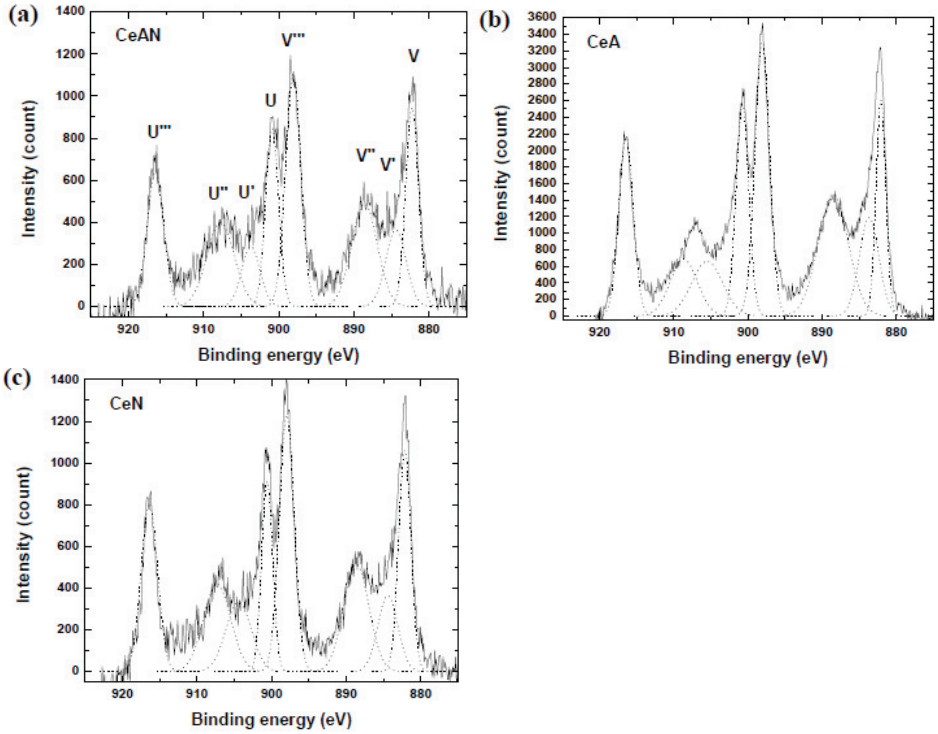


Fig. 4. Ce-3d spectra of the ceria particles from the precursors of (a) CeAN, (b) CeA and (c) CeN. Solid line represents the experimental spectrum (after background subtraction) and the dotted lines are the results with curve fitting.

## 4. Conclusions

The morphology of the ceria nanoparticles from CeAN, CeA and CeN precursors has been characterized using TEM imaging. Due to different solubilities of these three precursors, volume

precipitation, partial volume and surface precipitation and surface precipitation dominates the SP process to form main morphologies of spherical solid, hollow (closed and open pores) and porous (closed pores) of the ceria particles from CeAN and CeA and CeN precursors, respectively. Based on the result, by choosing suitable precursors, different morphological ceria particles can be obtained for different applications.

## Acknowledgements

The authors would like to thank you the financial support by National Science Council of Taiwan, ROC. (Grant No. NSC 99-2218-E-011-030-MY2) and by National Taiwan University of Science and Technology (Grant No. 100H451201).

## References

[1] Hennings U, Reimert R, Investigation of the structure and the redox behavior of gadolinium doped ceria to select a suitable composition for use as catalyst support in the steam reforming of natural gas. *Appl Catal A-Gen* 2007; 325:41-9.

[2] Cao CY, Cui ZM, Chen CQ, Song WG, Cai W, Ceria hollow nanospheres produced by a template-free microwave-assisted hydrothermal method for heavy metal ion removal and catalysis. *J Phys Chem C* 2010; 114:9865-70.

[3] Chen GZ, Zhu FF, Sun X, Sun SX, Chen RP, Benign synthesis of ceria hollow nanocrystals by a template-free method. *Cryst Eng Comm* 2011; 13:2904-8.

[4] Minh NQ, Ceramic fuel-cells. *J Am Ceram Soc* 1993; 76:563-88.

[5] Blumenth RN, Brugner FS, Garnier JE, Electrical conductivity of CaO-doped nonstoichiometric cerium dioxide from 700 $^{o}$C to 1500 $^{o}$C. *J Electrochem Soc* 1973; 120:1230-7.

[6] Rupp JLM, Drobek T, Rossi A, Gauckler LJ, Chemical analysis of spray pyrolysis gadolinia-doped ceria electrolyte thin films for solid oxide fuel cells. *Chem Mater* 2007; 19:1134-42.

[7] Phonthammachai N, Rumruangwong M, Gulari E, Jamieson AM, Jitkarnka S, Wongkasemjit S, Synthesis and rheological properties of mesoporous nanocrystalline $CeO_2$ via sol-gel process. *Colloid Surface A* 2004; 247:61-8.

[8] Masui T, Fujiwara K, Machida K, Adachi G, Sakata T, Mori H, Characterization of cerium(IV) oxide ultrafine particles prepared using reversed micelles. *Chem Mater* 1997; 9:2197-204.

[9] Bruce LA, Hoang M, Hughes AE, Turner TW, Surface area control during the synthesis and reduction of high area ceria catalyst supports. *Appl Catal A-Gen* 1996; 134:351-62.

[10] Madler L, Stark WJ, Pratsinis SE, Flame-made ceria nanoparticles. *J Mater Res* 2002; 17:1356-62.

[11] Kang HS, Kang YC, Koo HY, Ju SH, Kim DY, Hong SK et al., Nano-sized ceria particles prepared by spray pyrolysis using polymeric precursor solution. *Mat Sci Eng B-Solid* 2006; 127:99-104.

[12] Messing GL, Zhang SC, Jayanthi GV, Ceramic powder synthesis by spray-pyrolysis. *J Am Ceram Soc* 1993; 76:2707-26.

[13] Chen CY, Lyu YR, Su CY, Lin HM, Lin CK, Characterization of spray pyrolyzed manganese oxide powders deposited by electrophoretic deposition technique *Surf Coat Tech* 2007;202:1277-81.

[14] Zhang SC, Messing GL, Borden M, Synthesis of solid, spherical zirconia particles by spray pyrolysis. *J Am Ceram Soc* 1990; 73:61-7.

[15] Dubois B, Ruffier D, Odier P, Preparation of fien, spherical yttra-stabilized zirconia by the spray-pyrolysis method. *J Am Ceram Soc* 1989; 72:713-5.

[16] Shih SJ, Borisenko KB, Liu LJ, Chen CY, Multiporous ceria nanoparticles prepared by spray pyrolysis. *J Nanopart Res* 2010; 12:1553-9.

[17] Shih SJ, Herrero PR, Li G, Chen CY, Lozano-Perez S, Three-dimensional structures of mesoporous ceria particles using electron tomography. *Microsc Microanal* 2011; 17:54-60.

[18] Ishizawa H, Sakurai O, Mizutani N, Kato M, Homogeneous $Y_2O_3$-stabilized $ZrO_2$ powder by spary pyrolysis method. *Am Ceram Soc Bull* 1986; 65:1399-404.

[19] Xu HR, Gao L, Gu HC, Cuo JK, Yan DS, Synthesis of solid, spherical $CeO_2$ particles prepared by the spray hydrolysis reaction method. *J Am Ceram Soc* 2002; 85:139-44.

[20] Seidell A, *Solubilities of inorganic and organic substances*, New York, USA; D. Van Nostrand Company. 1919.

[21] Quill LL, Robey RF, The rare earth metals and their compounds. III. the ternary systems cerium group nitrates-nitric acid-water at 25 and 50$^o$. *J Amer Chem Soc* 1937; 59:2591-5.

[22] Kilbourn BT, *A lanthanide lantology. Mountain Pass: Molycorp Inc*; 1993.

[23] Vidal H, Kaspar J, Pijolat M, Colon G, Bernal S, Cordon A et al., Redox behavior of $CeO_2$-$ZrO_2$ mixed oxides I. Influence of redox treatments on high surface area catalysts. *Appl Catal B-Environ* 2000; 27:49-63.

[24] Shih SJ, Chang LYS, Chen CY, Borisenko KB, Cockayne DJH, Nanoscale yttrium distribution in yttrium-doped ceria powder. *J Nanopart Res* 2009; 11:2145-52.

[25] Shih SJ, Li G, Cockayne DJH, Borisenko KB, Mechanism of dopant distribution: an example of nickel-doped ceria nanoparticles. *Scripta Mater* 2009; 61:832-5.

[26] Shih SJ, Huang Y, Lyu YR, Chen CY, Cross-sectional observation of yttrium and nickel oxide doped ceria powder. *J Nanosci Nanotechnol* 2009; 9:3898-903.

[27] Burroughs P, Hamnett A, Orchard AF, Thornton G, Satellite structure in the X-ray photoelectron spectra of some binary and mixed oxides of lanthanum and cerium. *J Chem Soc Dalton Trans* 1976; 17:1686-98.

[28] Wang AQ, Punchaipetch P, Wallace RM, Golden TD, X-ray photoelectron spectroscopy study of electrodeposited nanostructured $CeO_2$ films. *J Vac Sci* 2003; 21:1169-75.

[29] El Fallah J, Hilaire L, Rome´o M, Le Normand F, Effect of surface treatments, photon and electron impacts on the ceria 3d core level. *J Electron Spectrosc Related Phenom* 1995; 73:89-103.